JOURNAL OF Materials CHEMISTRY

Synthesis of lithium manganese oxide in different lithium-containing fluxes

Xiaojing Yang,*[a] Weiping Tang,[b] Hirofumi Kanoh[a] and Kenta Ooi[a]

[a]*Shikoku National Industrial Research Institute, 2217-14 Hayashi-cho, Takamatsu-shi 761-0395, Japan. E-mail: yang@sniri.go.jp*
[b]*Research Institute for Solvothermal Technology, 2217-43 Hayashi-cho, Takamatsu-shi 761-0301, Japan*

Received 4th May 1999, Accepted 22nd July 1999

By using a needle-like raw material γ-MnOOH as a Mn-source, single crystals of lithium manganese oxides were synthesized in a variety of lithium-containing fluxes including $LiNO_3$, Li_2CO_3, LiOH, LiCl and Li_2SO_4. Needle-like $Li_{1.33}Mn_{1.67}O_4$ and Li_2MnO_3 crystals and plate-like polyhedral Li_2MnO_3 crystals were obtained in an $LiNO_3$ flux heated within different temperature ranges (300–400, 500–750 and 900–1000 °C, respectively). Not only polyhedral and film Li_2MnO_3 but also octahedral $LiMn_2O_4$ single crystals were obtained in an LiCl flux by use of different shaped containers to control the exposure to the atmosphere. Orthorhombic $LiMnO_2$ crystals with tube- and rod-like shapes could be obtained at the bottom of the LiCl melt at 1000 °C. The lithiation reaction (at low temperature) and dissolution–precipitation controlled growth (at high temperature) of Li_2MnO_3 were also observed in Li_2CO_3 and LiOH fluxes. According to the reaction mechanism, the Li-containing fluxes investigated can be classified into four types: (1) $LiNO_3$, oxidizing flux; (2) LiCl, non-oxide flux; (3) LiOH and Li_2CO_3, oxidic, but non-oxidizing fluxes; and (4) Li_2SO_4, no reaction.

1 Introduction

Porous and layered manganese oxide compounds are prepared *via* a variety of routes including solid state reaction, melting salt flux, redox precipitation, sol–gel, hydrothermal and hydrothermal soft chemical processes.[1,2] Different synthetic processes frequently give materials with different particle sizes and types and amounts of defects in the structures. These can result in materials with different ion exchange, catalytic and electrochemical properties. Preparation of single crystals is both scientifically and technically attractive. The flux growth technique is effective for growing some single crystals.

Only a few studies have been made on the flux growth synthesis of lithium manganese oxide. By using Mn_2O_3 as a Mn-source and LiOH, LiCl and LiCl–Li_2CO_3 as fluxes, Strobel *et al.*[3] found that only Li_2MnO_3 forms in all the fluxes when heated in air in a muffle furnace. In an Li_2CO_3–K_2CO_3 eutectic melt, $LiMnO_2$ or Li_2MnO_3 (according to the partial pressure of CO_2) was found as the stable phase.[4] In our laboratory, Tang *et al.* have synthesized single crystals of $LiMnO_2$ and Li_2MnO_3,[5,6] as well as Li_2MnO_3 single crystal films[7] in a flux of LiCl (LiCl–LiOH for $LiMnO_2$) by controlling the atmosphere in the furnace.

In this study, various lithium-containing fluxes were selected in order to investigate the influence of the oxidizing power of different fluxes on manganese valency, and consequently on the crystal products in air. The decomposition of manganese oxide in air in different temperature ranges[8,9] shows that lower valence Mn ions are thermochemically more stable than higher valence ions at high temperature. Hence, to clarify the temperature range for crystals to be stable, fluxes were heated at various temperatures between a temperature higher than T_m (the melting point of a flux) and 1000 °C.

2 Experimental

LiCl, $LiNO_3$, Li_2SO_4, Li_2CO_3 and LiOH were selected as fluxes. All reagents (LiCl, $LiNO_3$, $Li_2SO_4 \cdot H_2O$, Li_2CO_3 and $LiOH \cdot H_2O$, reagent grade) were obtained from Wako Pure Chemical Industries, Ltd. (Japan). γ-MnOOH used as the Mn-source was purchased from Toyo Soda Manufacturing Co., Ltd. (Japan) (Mn, 62.54; H_2O, 0.35; Fe, 0.012; SiO_2, 0.01; SO_4^{2-}, 0.49 wt%). Its morphology is shown in Fig. 1.

In an air atmosphere, γ-MnOOH is decomposed to β-MnO_2 at 220 °C, and the latter phase is further reduced to α-Mn_2O_3 at 550 °C.[9] α-Mn_2O_3 decomposes into tetragonal Mn_3O_4 at 850–900 °C.[8] The formation of β-MnO_2 proceeds in two successive stages [eqn. (1) and (2)].[9]

$$2MnOOH \rightarrow Mn_2O_3 + H_2O \quad (1)$$

$$Mn_2O_3 + 1/2O_2 \rightarrow 2MnO_2 \quad (2)$$

Considering these temperature ranges, the fluxes were heated at 300, 400, 500, 650, 750, 900 and 1000 °C. Because oxygen is necessary for the increase in valency of manganese, and to observe the effect of air on the reaction, two types of containers were used. One was a pure alumina crucible cover (diameter

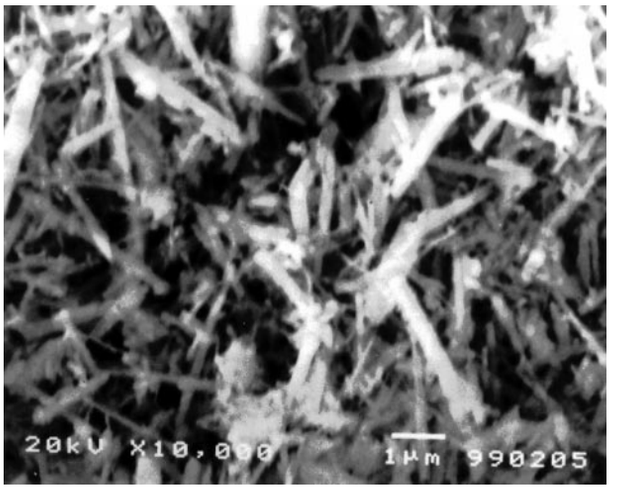

Fig. 1 SEM micrograph showing the morphology of the raw material γ-MnOOH.

85 mm) used as a dish, and the other was a pure alumina crucible (50 ml). The former was wide open to the air, while the latter was covered with a cap when heated.

γ-MnOOH (1 g) and the Li-containing raw material were mixed together in the molar ratio of Mn/Li = 1/17, and placed into the container. The mixture was heated in a muffle furnace for 24 h in most cases, and then cooled to room temperature in the furnace. Crystals obtained were washed with distilled water several times, filtered through filter paper of 0.45 μm pore size, and dried at 70 °C.

The lithium and manganese contents in the individual samples were determined by atomic absorption analysis after being dissolved in a mixed solution of HCl and H_2O_2. The formulae of some crystals were calculated from the results of the atomic absorption analysis and an available oxygen analysis carried out by the standard oxalic acid method as described in ref. 10. X-Ray diffraction (XRD) data were collected on a Rigaku RINT 1200 powder diffractometer using Cu-Kα radiation. Microscopic observations were performed in a JEOL type JSM-5310 and a Hitachi type S-246N scanning electron microscope (SEM).

3 Results and discussion

Crystal phases and chemical analysis results are summarized in Table 1. The XRD patterns of Li_2MnO_3 in Table 1 were identified by comparison with JCPDS card 27-1252, and $LiMn_2O_4$ with card 35-0782, β-MnO_2 with card 24-0735, and Mn_2O_3 and Mn_3O_4 in Li_2SO_4 with cards 31-825 and 24-0734, respectively. All synthesized single crystal samples had Li/Mn ratios close to stoichiometric, except those from LiOH and Li_2CO_3 fluxes. Only the LiCl flux yielded different crystal phases in the two different containers, indicating that in this flux, the reaction of the manganese oxide with LiCl was very sensitive to the atmosphere. Li_2MnO_3 was a stable phase even within the temperature range 750–1000 °C, over which Mn^{3+} is stable at the lower end and $Mn^{2+} + Mn^{3+}$ at the upper end in air.

The color of Li_2MnO_3 crystal samples changes from ochre to orange and then to red with increasing temperature. This change in color is similar to the result described by Jansen and Hoppe.[11]

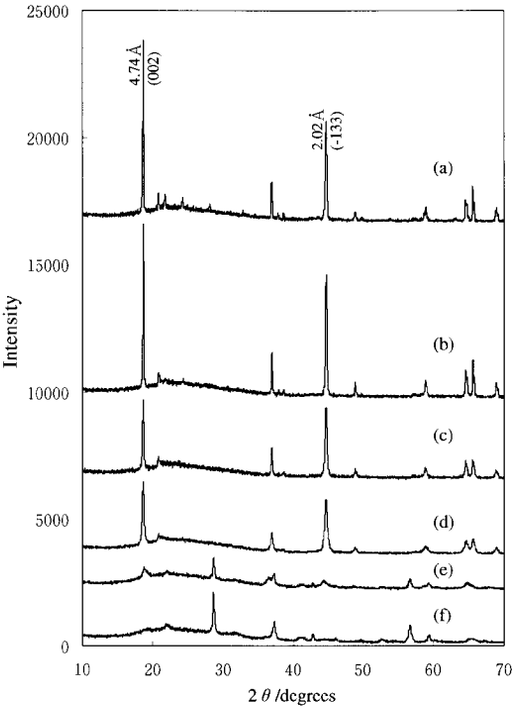

Fig. 2 XRD patterns of the samples obtained in an $LiNO_3$ flux heated at (a) 1000, (b) 900, (c) 750, (d) 500, (e) 400 and (f) 300 °C for 24 h in a covered crucible.

3.1 $LiNO_3$ flux

Fig. 2 shows the XRD patterns of the samples in an $LiNO_3$ flux heated at different temperatures for 24 h in a crucible. The same patterns were observed for the samples obtained in a dish. The patterns for the samples heated at temperatures >400 °C were readily identifiable as Li_2MnO_3. The chemically analyzed formula of the sample heated at 500 °C was $Li_{1.88}MnO_{2.91}$ while that at 900 °C was $Li_{1.98}MnO_{2.97}$. The patterns for samples heated at 300 and 400 °C could be assigned as a mixture of a spinel phase (discussed below) and β-MnO_2. Fig. 3 shows SEM micrographs of these crystals. At high temperature (1000 and 900 °C), the crystals grew in the

Table 1 Results of crystal phases and atomic absorption analysis

		Heated in a crucible			Heated in a cover		
Flux	Heating temperature[a]/°C	Crystal phase	Li/Mn	Color	Crystal phase	Li/Mn	Color
$LiNO_3$	300	$Li_{1.33}Mn_{1.67}O_4$	—	Black	$Li_{1.33}Mn_{1.67}O_4$	—	Black
	400	β-MnO_2	0.82[b]	Black	β-MnO_2	—	Black
	500	Li_2MnO_3	1.88	Ochre	Li_2MnO_3	2.00	Ochre
	750		1.89	Orange		1.93	Orange
	900		1.98	Orange		1.96	Orange
	1000		2.05	Red		2.04	Red
LiCl	650	$LiMn_2O_4$	0.52	Red	Li_2MnO_3	1.72	Red
	750		0.48	Red		1.99	Red
	900		0.45	Deep-red		1.84	Deep-red
	1000	$LiMn_2O_4$	0.34	Black	Mn_2O_3	—	Black
		$LiMnO_2$	0.82	Black	Li_2MnO_3		
LiOH	500	Li_2MnO_3	1.88	Ochre	Li_2MnO_3	2.29	Ochre
	750		3.28[c]	Orange		2.42	Orange
	900		3.07[c]	Red		2.24	Red
	1000		3.01[c]	Red		2.76[c]	Red
Li_2CO_3	750	Li_2MnO_3	1.83	Ochre	Li_2MnO_3	2.09	Ochre
	900		2.10	Orange		2.20	Orange
	1000		3.21[c]	Orange–red		2.30	Orange–red
Li_2SO_4	900	Mn_2O_3	—	Black	Mn_2O_3	—	Black
	1000	Minor phase: Mn_3O_4	—	Black	Minor phase: Mn_3O_4	—	Black

[a]24 h. [b]Analyzed for the sample heated for 168 h. [c]$LiAlO_2$ was detected, which is the probable cause of the large Li/Mn ratio.

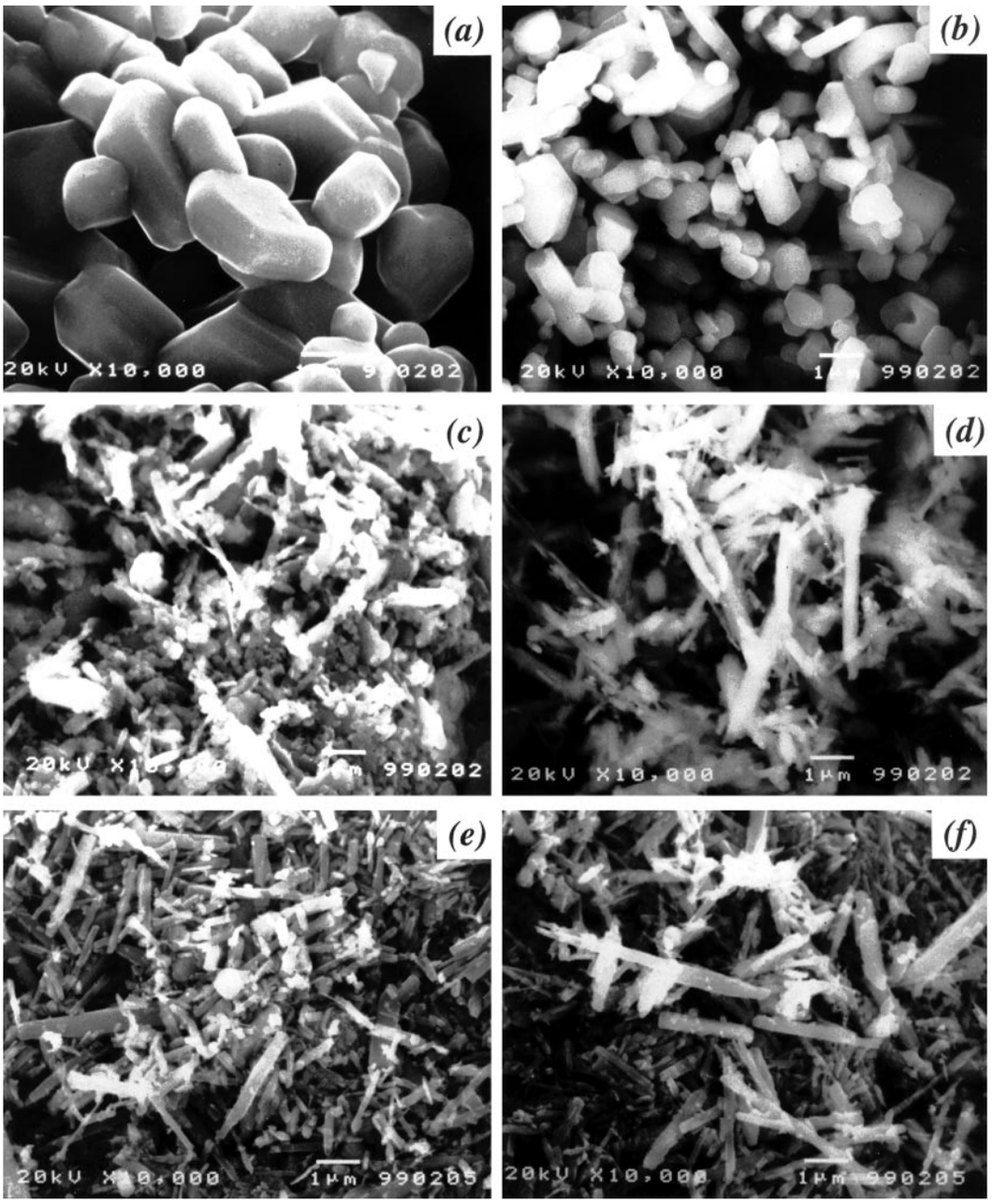

Fig. 3 SEM micrographs showing the morphology of the crystals obtained in an $LiNO_3$ flux heated at (a) 1000, (b) 900, (c) 750, (d) 500, (e) 400 and (f) 300 °C for 24 h in a covered crucible.

shape of plate-like polyhedra as shown in Fig. 3(a) and (b), respectively. This indicates that the growth of Li_2MnO_3 at high temperature is controlled by a dissolution–precipitation process. At low temperature (300–750 °C), the crystals adopted the same needle-like shape as that of γ-MnOOH (Fig. 1) as shown in Fig. 3(c)–(f). This testifies that a lithiation reaction occurred at low temperature without any morphology change. It can be concluded that because of differences of the crystal shape, different reaction mechanisms occur in the $LiNO_3$ melt: a lithiation reaction process at low temperature, and a dissolution–precipitation process at high temperature.

As shown in Fig. 2(a) and (b), the intensity ratio of the (002) peak to the (−133) peak in the XRD patterns, I_{002}/I_{-133}, was high for the samples of plate-like Li_2MnO_3 crystals [Fig. 3(a) and (b)]. Conversely, the peak due to the (−133) plane was relatively high for needle-like Li_2MnO_3 crystals obtained at 500 and 750 °C. These results indicate that, in accordance with its crystal habit, the Li_2MnO_3 crystal shows relatively rapid growth of the (002) plane when its growth is dissolution–precipitation-controlled.

Because $LiNO_3$ decomposes according to eqn. (3) over the temperature range 500–1000 °C, the reaction in the $LiNO_3$ flux can be suggested to be given by eqn. (4).

$$2LiNO_3 \rightarrow Li_2O + 2NO_2 + 1/2O_2 \quad (3)$$

$$2LiNO_3 + MnOOH \rightarrow Li_2MnO_3 + 2NO_2 + 1/2H_2O + 1/4O_2 \quad (4)$$

From this reaction, it is obvious that external oxygen is not necessary for Li_2MnO_3 to crystallize. When the heating temperature is higher than the decomposition temperature of $LiNO_3$ (600 °C)[12] excess oxygen in the melt readily oxidizes Mn^{3+} to Mn^{4+} to form Li_2MnO_3.

Fig. 4 shows XRD results for the samples heated at 400 °C for various lengths of time. The color of the product changed

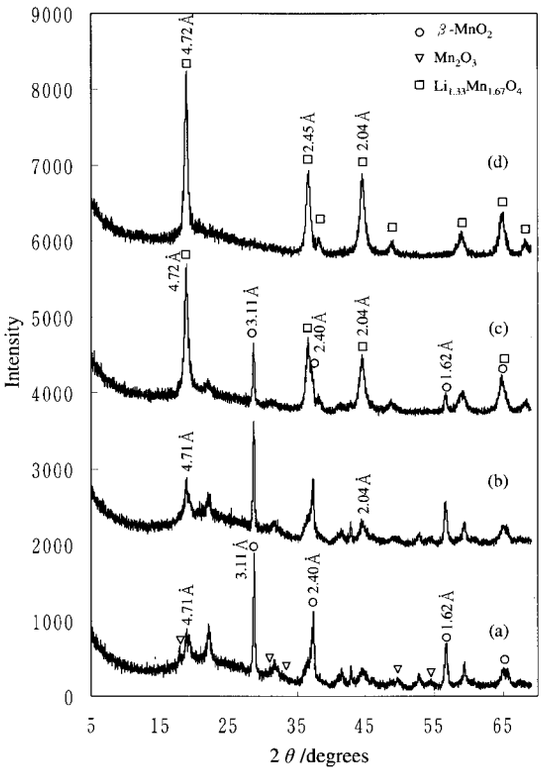

Fig. 4 XRD patterns of the samples prepared in an $LiNO_3$ flux heated at 400 °C for (a) 4, (b) 12, (c) 60 and (d) 168 h.

from black to blackish brown with an increase of heating time from 4 to 168 h. For the samples heated for 4 and 12 h in Fig. 4, β-MnO_2 was the main crystal phase while small peaks due to Mn_2O_3 and peaks at $d=4.7$ and 2.0 Å were observed. The intensity of the β-MnO_2 peaks decreased with increasing heating time while the peaks at $d=4.7$ and 2.0 Å increased in

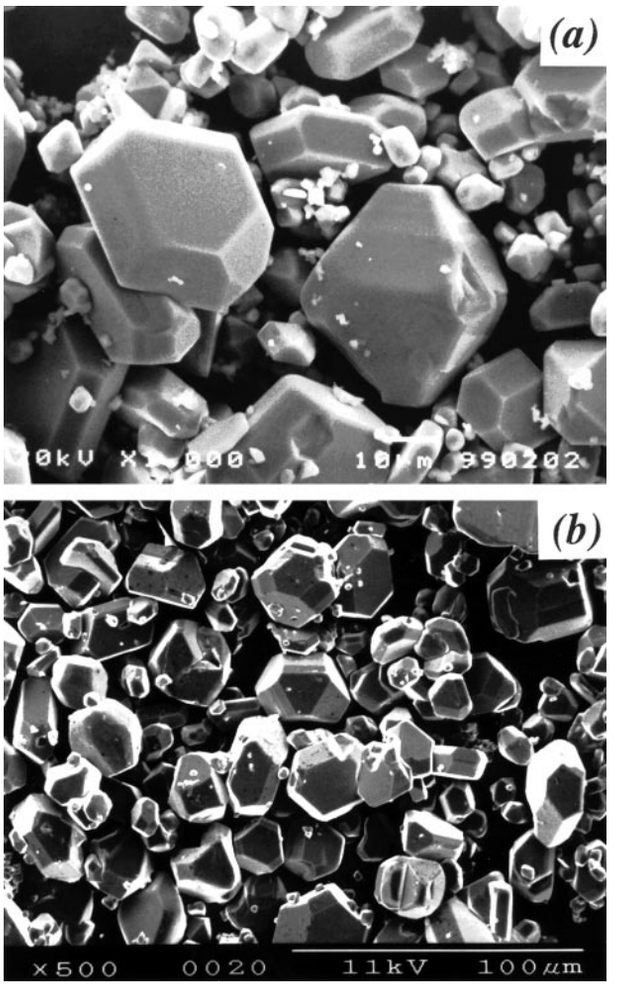

Fig. 6 SEM micrographs of Li_2MnO_3 obtained in an LiCl flux heated at (a) 750 and (b) 650 °C for 24 h in an open dish.

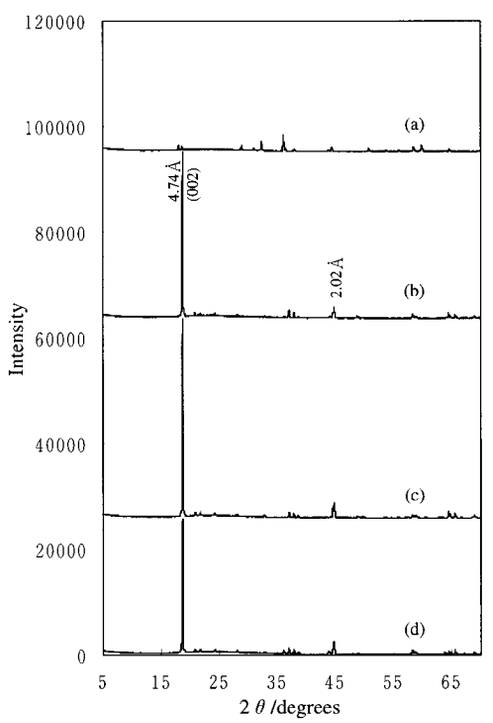

Fig. 5 XRD patterns of the samples obtained in an LiCl flux heated at (a) 1000, (b) 900, (c) 750 and (d) 650 °C for 24 h in a dish wide open to air.

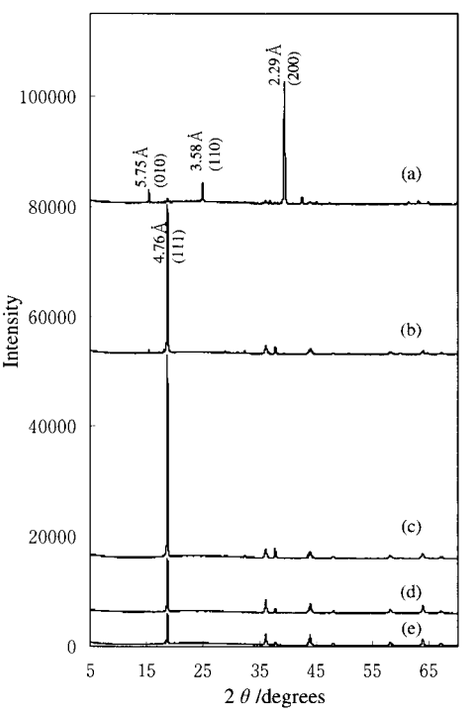

Fig. 7 XRD patterns of the samples obtained in an LiCl flux in a covered crucible heated at (a) 1000 °C, large particles at the bottom of the crucible; (b) 1000 °C, small particles; and (c) 900, (d) 750 and (e) 650 °C for 24 h.

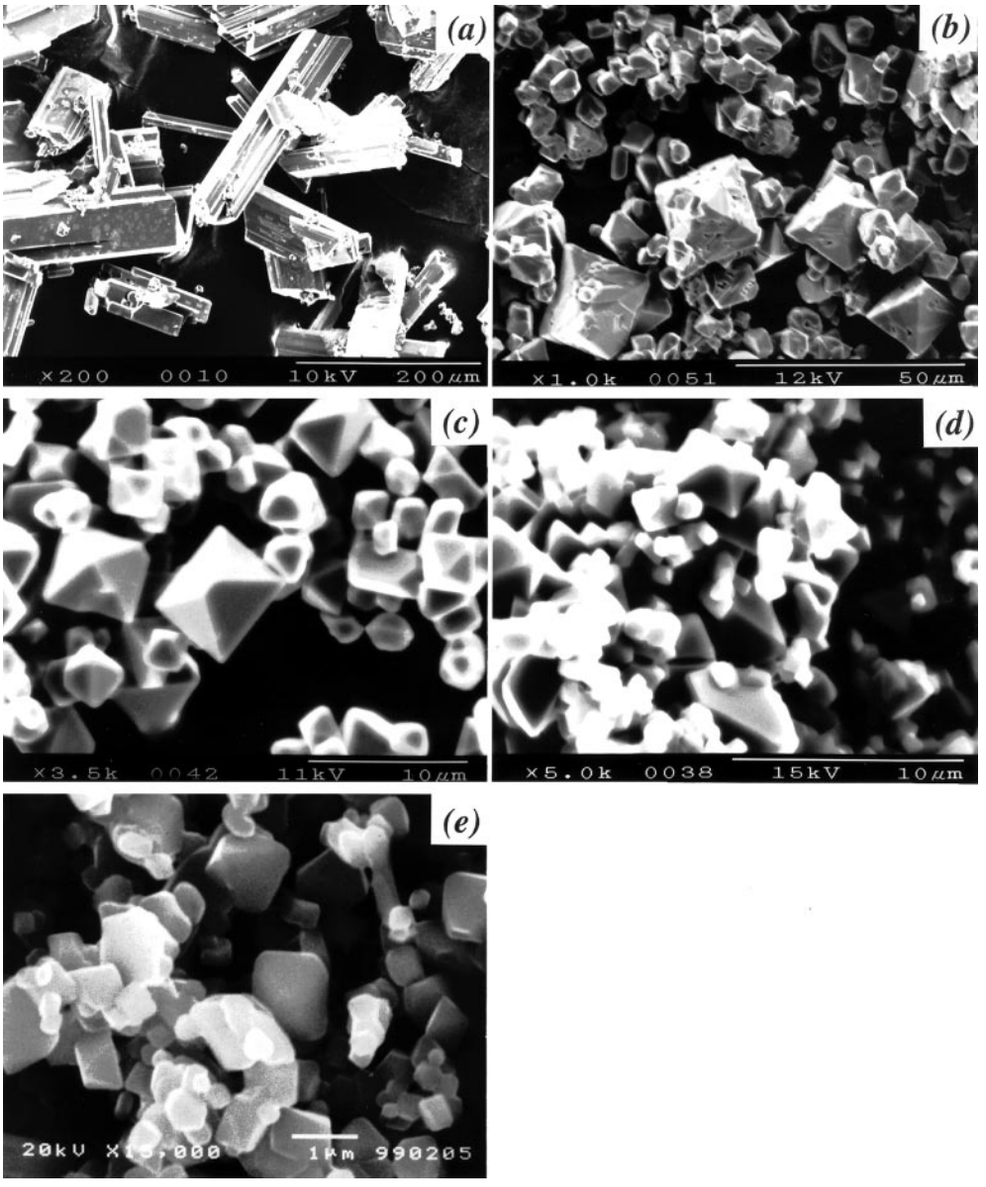

Fig. 8 SEM micrographs of (a) orthorhombic $LiMnO_2$ and (b)–(e) cubic $LiMn_2O_4$ obtained in an LiCl flux heated at (a) and (b) 1000, (c) 900, (d) 750 and (e) 650 °C for 24 h in a covered crucible.

intensity. These increasing peaks are difficult to identify, because of the close similarity in the XRD patterns of Li_2MnO_3 and the spinel phase.[13] However, it is always found that the lithiation of MnO_2 gives rise to products from which the $LiMn_2O_4$ spinel is formed upon heating.[14] Using atomic absorption analysis and standard oxalic acid analysis, the formula of the sample heated for 168 h was determined as $Li_{1.38}Mn_{1.69}O_4$. These results indicate the formation of $Li_{1.33}Mn_{1.67}O_4$ (*i.e.* $Li_4Mn_5O_{12}$)[10,15] in spinel form as a result of the insertion of Li^+ into the β-MnO_2 structure. The lithiation reaction of β-MnO_2 can be written in terms of eqn. (5).

$$4LiNO_3 + 5MnO_2 \rightarrow Li_4Mn_5O_{12} + 4NO_2 + O_2 \qquad (5)$$

The formation of needle-like Li_2MnO_3 crystals at 500 °C [Fig. 3(d)] is also due to the lithiation reaction. David *et al.*[16] have suggested a model for the transformation mechanism, on lithiation, from the β-MnO_2 framework to the $[Mn_2]O_4$ framework of a spinel phase. According to this model, the conservation of morphology between β-MnO_2 and the spinel phase is readily rationalized. If we consider that γ-MnOOH has approximately the same one-dimensional (1×1) tunnel structural feature as pyrolusite (β-MnO_2),[2,17,18] we may rationalize the conservation of morphology between γ-MnOOH and β-MnO_2. However, there is no model to describe the lithiation of β-MnO_2 to form Li_2MnO_3 with rocksalt structure. Further work is needed to clarify directly the relation between morphology and phase restructuring during the lithiation reaction.

3.2 LiCl flux

In an LiCl flux, different products were obtained according to the container used. In an open dish, the LiCl flux yielded Li_2MnO_3 when heated in the range 650–900 °C, as shown in Fig. 5. At 1000 °C, Mn_2O_3 was the main crystal phase, though some Li_2MnO_3 peaks are observed in Fig. 5(a). SEM photographs for the samples heated at 650 and 750 °C are shown in Fig. 6. A significant amount of Li_2MnO_3 film was obtained, as reported previously.[6,7] The polyhedral shape of the crystals in Fig. 6 differs from that obtained in the $LiNO_3$ flux (Fig. 3). Li_2MnO_3 crystals from an LiCl flux had a much higher I_{002}/I_{-133} ratio in their XRD patterns [Fig. 5(b)–(d)] than did the plate- and needle-like crystals of Li_2MnO_3 from an $LiNO_3$ flux (Fig. 2).

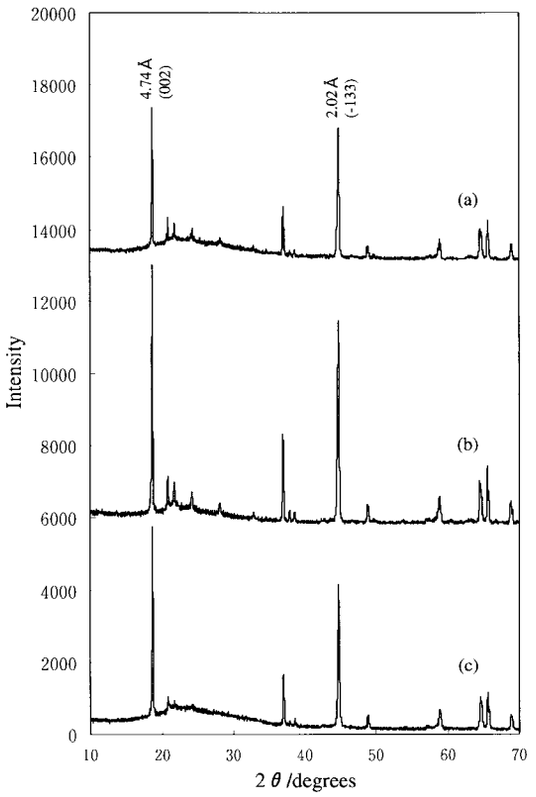

Fig. 9 XRD patterns of the samples obtained in an Li_2CO_3 flux heated at (a) 1000, (b) 900 and (c) 750 °C for 24 h in a crucible.

Fig. 7 and 8 show the XRD and SEM results for samples obtained in the covered crucible. $LiMn_2O_4$ single crystals were of octahedral shape (Fig. 8). Fig. 7 shows that the (111) plane of this crystal grew quickly with increasing temperature and large octahedra can be observed at 900 °C [Fig. 8(c)]. However, at 1000 °C [Fig. 8(b)] there were some holes in the surfaces of the crystals which may be due to crystals growing too quickly and leading to defects. $LiMnO_2$ crystals from the bottom of the crucible heated at 1000 °C were obtained in tube- and rod-like shapes as shown in Fig. 8(a).

In a wide open container, the liquid (solid)–atmosphere interface is suitable for Li_2MnO_3 growth and reactions (6) and (7) occur to form Li_2MnO_3.[6]

$$LiCl + 2MnOOH + 1/4O_2(air) \rightarrow LiMn_2O_4 + 1/2H_2O + HCl \quad (6)$$

$$3/2LiCl + 1/2LiMn_2O_4 + 1/2O_2(air) \rightarrow Li_2MnO_3 + 3/4Cl_2 \quad (7)$$

Reactions (6) and (7) show that the crystallization of Li_2MnO_3 and $LiMn_2O_4$ is controlled by the diffusion of O^{2-} ions in the melt. Therefore in a covered crucible, relatively less oxygen results in only $LiMn_2O_4$ *via* reaction (6). At the bottom of the LiCl melt, oxygen is scarce and $LiMnO_2$ forms according to reaction (8).

$$LiCl + MnOOH \rightarrow LiMnO_2 + HCl \quad (8)$$

3.3 Li_2CO_3 and LiOH fluxes

Fig. 9 and 10 show XRD patterns and SEM photographs, respectively, of the crystals obtained from an Li_2CO_3 flux, and Fig. 11 and 12 those from a LiOH flux. $LiAlO_2$ was detected from XRD peaks shown in Fig. 11 and is due to the attack of LiOH on the alumina container. This impurity is the probable cause of the observed large Li/Mn ratio (Table 1).

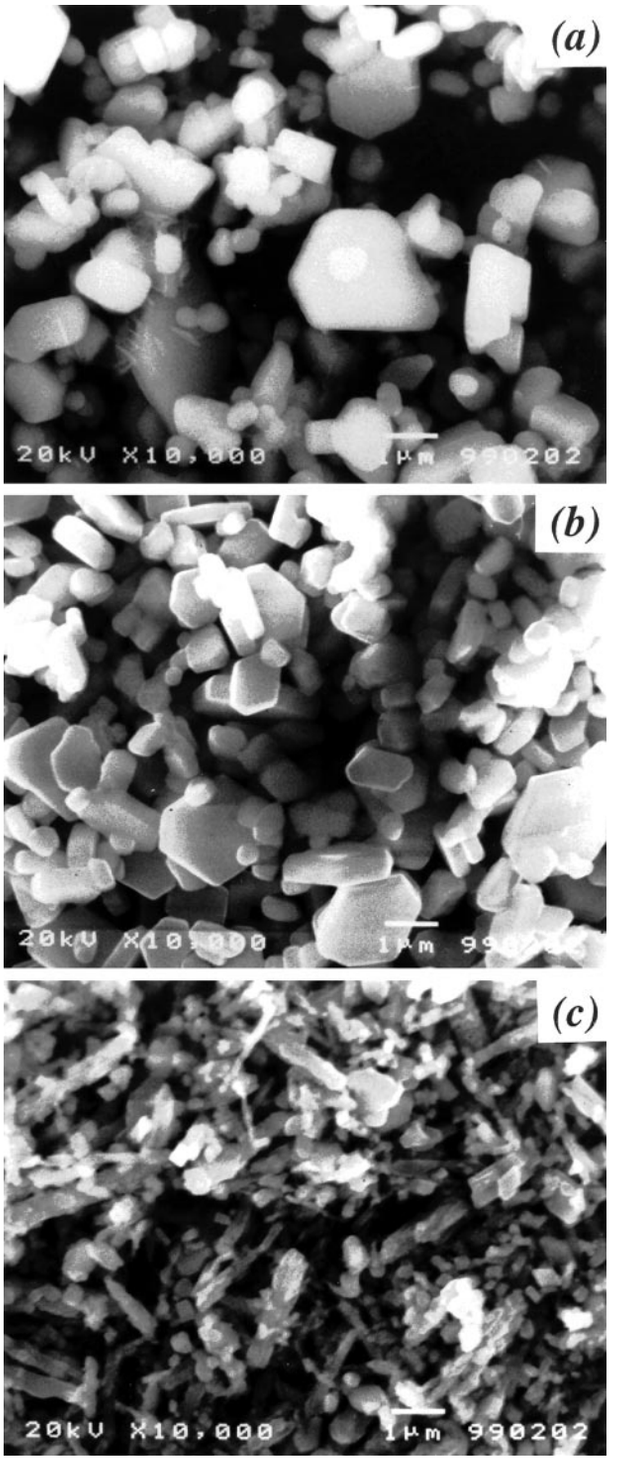

Fig. 10 SEM micrographs of Li_2MnO_3 obtained in an Li_2CO_3 flux heated at (a) 1000, (b) 900 and (c) 750 °C for 24 h in a crucible.

The decomposition of Li_2CO_3 in air is given by eqn. (9),[19] and the total reaction in the Li_2CO_3 flux may be expressed as eqn. (10).

$$Li_2CO_3 \rightarrow Li_2O + CO_2 \quad (9)$$

$$Li_2CO_3 + MnOOH + 1/4O_2(air) \rightarrow Li_2MnO_3 + CO_2 + 1/2H_2O \quad (10)$$

The dissolution–precipitation process controls the crystal growth as shown in Fig. 10(a) and (b), but in Fig. 10(c), the needle-like shape, which differs from that in Fig. 1, is a consequence of the lithiation reaction. This indicates that at

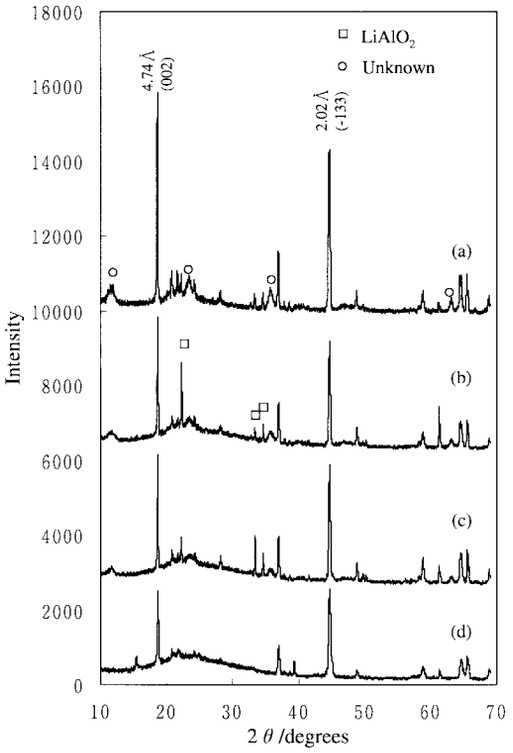

Fig. 11 XRD patterns of samples obtained in an LiOH flux heated at (a) 1000, (b) 900, (c) 750 and (d) 500 °C for 24 h in a crucible.

low temperature (750 °C), the crystallization of Li_2MnO_3 is primarily *via* a lithiation reaction and successively controlled by a dissolution–precipitation process. It should be noted that owing to the lithiation reaction, a nucleation process in the usual sense is not needed for Li_2MnO_3 crystallization, at least in a low temperature range.

In an LiOH flux, external oxygen is also necessary for the formation of Li_2MnO_3 as shown in eqn. (11):

$$2LiOH + MnOOH + 1/4O_2(air) \rightarrow Li_2MnO_3 + 3/2H_2O \quad (11)$$

When the temperature is higher than 924 °C, LiOH decomposes according to eqn. (12).[19]

$$2LiOH \rightarrow Li_2O + H_2O \quad (12)$$

Fig. 12(d) shows needle-shaped crystals which are direct evidence for the lithiation reaction. This lithiation reaction would induce reaction of LiOH with manganese oxide *via* eqn. (11). However, the plate-shaped crystals [Fig. 12(c)] obtained at 750 °C (lower than the decomposition temperature of LiOH) indicate the growth of Li_2MnO_3 by a dissolution–precipitation process, *i.e.* eqn. (11) also proceeds *via* a dissolution–precipitation process.

3.4 Li_2SO_4 flux

As indicated in Table 1, no lithium manganese oxide formed at 900 or 1000 °C in the Li_2SO_4 flux, *i.e.* Li_2SO_4 did not react with manganese oxide. Unlike in air, Mn_2O_3 remains stable in the Li_2SO_4 flux as the main crystal phase even at 1000 °C.

3.5 Effect of oxygen diffusion in melts

The growth of Li_2MnO_3 crystals depends on the diffusion of external oxygen in the LiCl melt in which there is no internal oxygen. No lithiation reaction was found in the LiCl flux. It is possible to control the valence of Mn ions by varying the atmosphere. In this way, $LiMn_2O_4$ and $LiMnO_2$ were obtained from fluxes heated in covered crucibles. $LiNO_3$, which can release oxygen on heating, yielded the same crystal phases in both a covered container and a wide open container, while $Li_{1.33}Mn_{1.67}O_4$ and Li_2MnO_3 were obtained *via* the lithiation reaction in an $LiNO_3$ flux at low temperature (300–750 °C).

In both the LiOH and Li_2CO_3 fluxes, the lithiation reaction was also observed. To form one mole of Li_2MnO_3, the amount

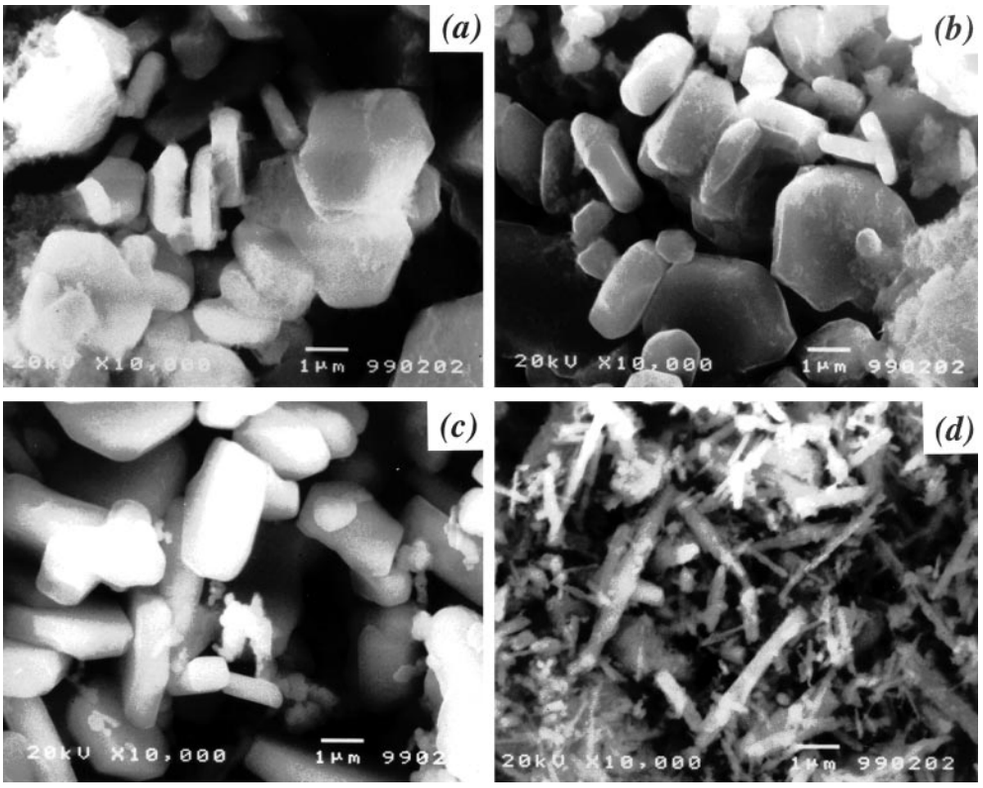

Fig. 12 SEM photographs of Li_2MnO_3 obtained in an LiOH flux fired at (a) 1000, (b) 900, (c) 750 and (d) 500 °C for 24 h in a crucible.

of external oxygen required is only two fifths of that in an LiCl flux [*cf.* reactions (10) and (11) with (6) and (7)]. The internal oxygen in LiOH and Li_2CO_3 fluxes leads to the same lithiation reaction as in the $LiNO_3$ flux. The same crystal phases were obtained in each type of container (Table 1), and the SEM micrographs showed no obvious differences between them. Thus, by the use of a mixture of LiOH and LiCl as a flux,[5] $LiMnO_2$ crystals could be obtained.

4 Conclusion

In an $LiNO_3$ flux, $Li_{1.33}Mn_{1.67}O_4$ and Li_2MnO_3 can be obtained at different temperatures. Needle-like spinel ($Li_{1.33}Mn_{1.67}O_4$) crystals, which retained the shape of the Mn-source raw material γ-MnOOH, can be obtained at low temperature (300 and 400 °C) in an $LiNO_3$ melt. The crystallization of the spinel is controlled by the lithiation reaction of β-MnO_2. On heating at 500–750 °C for 24 h, the $LiNO_3$ flux yielded Li_2MnO_3 crystals with the same needle-like shape as the raw material and indicates that the lithiation reaction controls growth. At high temperatures (900 and 1000 °C), the relatively quick growth of the (002) plane (as shown in XRD patterns) led the Li_2MnO_3 single crystals to form plate-like polyhedra and shows that the dissolution–precipitation process controls the growth. The manner in which the lithiation reaction (at low temperature) and the dissolution–precipitation reaction (at high temperature) controlled the growth of Li_2MnO_3 is also observed in Li_2CO_3 and LiOH fluxes. Further study is needed to clarify the relationship between morphology and phase restructuring during the lithiation reaction.

Using different shaped containers to control exposure to the atmosphere, not only polyhedral and film Li_2MnO_3 but also octahedral $LiMn_2O_4$ single crystals were formed in the LiClflux. Tube- and rod-like $LiMnO_2$ crystals were obtained at the bottom of the LiCl melt at 1000 °C.

According to the mechanism of the reaction of an Li-containing flux with γ-MnOOH to form lithium manganese oxide crystals, the Li-containing fluxes investigated can be classified into four types: (1) $LiNO_3$, oxidizing flux, in which a lithiation reaction occurs at low temperature; (2) LiCl, non-oxide flux in which O^{2-} ion diffusion in the melt is important; (3) LiOH and Li_2CO_3, oxidic, but non-oxidizing fluxes with behavior intermediate between cases (1) and (2); and (4) Li_2SO_4, in which no reaction occurs.

References

1 S. L. Brock, N. Duan, Z. R. Tian, O. Giraldo, H. Zhou and S. L. Suib, *Chem. Mater.*, 1998, **10**, 2619.
2 Q. Feng, H. Kanoh and K. Ooi, *J. Mater. Chem.*, 1999, **9**, 319.
3 P. Strobel, J-P. Levy and J-C. Joubert, *J. Cryst. Growth*, 1984, **66**, 257.
4 K. Ota, M. Nakamura, H. Yokokawa, H. Yoshitake, Y. Abe and N. Kamiya, *Denki Kagaku*, 1994, **62**, 165.
5 W. Tang, H. Kanoh and K. Ooi, *J. Solid State Chem.*, 1999, **142**, 19.
6 W. Tang, H. Kanoh and K. Ooi, in *Symposium at the 9th Meeting of the Materials Research Society of Japan*, The Materials Research Society of Japan, Kawasaki-shi KSP, 1997, p. 81.
7 W. Tang, H. Kanoh and K. Ooi, *Jpn. Pat.*, No.9-218898, 9-270192, 1997.
8 R. D. W. Kemmitt, in *Comprehensive Inorganic Chemistry*, ed. J. C. Bailar, Jr., H. J. Emeleus, S. R. Nyholm and A. F. Trotman-Dickenson, Pergamon, Oxford, 1973, p. 772.
9 M. Sato, K. Matsuki, M. Sugawara and T. Endo, *Nippon Kagaku Kaishi*, 1973, **9**, 1655 (in Japanese).
10 Q. Feng, Y. Miyai, H. Kanoh and K. Ooi, *Langmuir*, 1992, **8**, 1861.
11 V. M. Jansen and R. Hoppe, *Z. Anorg. Allg. Chem.*, 1973, **397**, 279.
12 The Chemical Society of Japan, *Kagaku Binran, Kiso-hen-II*, Maruzen, Tokyo, 1984 (in Japanese).
13 G. Blasse, *Philips Res. Rep., Suppl.*, 1964, **3**, 1.
14 M. H. Rossouw, A. de Kock, L. A. de Picciotto, M. M. Thackeray, W. I. F. David and R. M. Ibberson, *Mater. Res. Bull.*, 1990, **25**, 173.
15 G. Pistoia, A. Antonini, D. Zane and M. Pasquali, *J. Power Sources*, 1995, **56**, 37.
16 W. I. F. David, M. M. Thackeray, P. G. Bruce and J. B. Goodenough, *Mater. Res. Bull.*, 1984, **19**, 99.
17 L. A. H. MacLean, C. Poinsignon, J. M. Amarilla, F. L. Cras and P. Strobel, *J. Mater. Chem.*, 1995, **5**, 1183.
18 R. G. Burns and V. M. Burns, in *Manganese Dioxide Symposium*, ed. B. Schumm, Jr., H. M. Joseph and A. Kozawa, I. C. MnO_2 Sample Office, Ohio, 1981, vol. 2, p. 97.
19 O. Knacke, O. Kubaschewski and K. Hesselmann, *Thermochemical Properties of Inorganic Substances*, Springer-Verlag, Berlin, 2nd edn., 1991.

Paper 9/03495A